Signal Processing 89 (2009) 1050–1060

Contents lists available at ScienceDirect

Signal Processing

journal homepage: www.elsevier.com/locate/sigpro

Second and fourth order statistics-based reduced polynomial rooting direction finding algorithms

Wasyl Wasylkiwskyj [a], Ivica Kopriva [b,*]

[a] Department of Electrical and Computer Engineering, The George Washington University, 801 22nd Street, NW Room 615, Washington, DC 20052, USA
[b] Rudjer Boskovich Institute, Bijenicka cesta 54, 10002 Zagreb, Croatia

ARTICLE INFO

Article history:
Received 4 April 2008
Received in revised form
10 November 2008
Accepted 8 December 2008
Available online 24 December 2008

Keywords:
Direction finding
Polynomial rooting algorithms
Second order statistics
Fourth order statistics

ABSTRACT

Polynomial rooting direction finding (DF) algorithms are a computationally efficient alternative to search-based DF algorithms and are particularly suitable for uniform linear arrays (ULA) of physically identical elements provided mutual interaction among the array elements can be either neglected or compensated for. A popular polynomial rooting algorithm is Root-MUSIC (RM) wherein, for an N-element array, the estimation of the directions of arrivals (DOA) requires the computation of the roots of a $2N-2$-order polynomial for a second order (SO) statistics- and a $4N-4$-order polynomial for a fourth order (FO) statistics-based approach, wherein the DOA are estimated from L pairs of roots closest to the unit circle, when L signals are incident on the array. We derive SO- and FO statistics reduced polynomial rooting (RPR) algorithms capable to estimate L DOA from L roots only. We demonstrate numerically that the RPR algorithms are at least as accurate as the RM algorithms. Simplified algebraic structure of RPR algorithms leads to better performance than afforded by RM algorithms in saturated array environment, especially in the case of FO methods when number of incident signals exceeds number of elements and under low SNR and/or small sample size conditions.

1. Introduction

Super-resolution direction finding (DF) algorithms for linear arrays fall into two broad categories: search-based algorithms, as exemplified by MUSIC [1,2] and root-based algorithms such as Root-MUSIC (RM) [3,4], ESPRIT [2]. Search algorithms make no assumptions about the algebraic structure of the array steering vectors but require that they be known to great accuracy, especially if a high degree of angular resolution is called for. In that case they can also be computationally quite demanding. In practice the determination of the array steering vector amounts to an accurate measurement of the magnitude and phase of the array element patterns, sometimes referred to as array manifold calibration. Normal accuracies attained in such measurements are a few tenths of a dB in amplitude and about 1° in phase, which generally is insufficient for the design of high-resolution DF systems. Admittedly an alternative technique would be to rely on numerical computer simulations (either computing the element patterns directly or inferring them from the array geometry and the computed impedance or scattering matrix). However our experience with comparisons of numerical simulations using the latest commercially available software with experimental data indicates that presently this is not yet a fruitful approach [5].

Root-based algorithms on the other hand require no array calibration and afford substantial computational efficiency over search algorithms. They require that the elements be uniformly spaced and physically identical, which a search algorithm such as MUSIC does not. The

* Corresponding author.
E-mail addresses: wasylkiw@gwu.edu (W. Wasylkiwskyj), ikopriva@irb.hr (I. Kopriva).

0165-1684/$ - see front matter © 2009 Elsevier B.V. All rights reserved.
doi:10.1016/j.sigpro.2008.12.004

more significant restriction, however, is that the array steering vector must have the form of an array factor of a linear array of uniformly spaced elements. Unfortunately due to inter-element mutual coupling this idealized form of the steering vector is practically unattainable without compensation. Indeed, when root-based DF algorithms are applied to a real array without some form of compensation, significant angle estimation errors can result [6]. Compensation for the effects of mutual coupling can be realized by employing extra "dummy" elements to equalize the active element radiation patterns [7,8]. Under the assumption that the element radiation patterns are sufficiently equalized, the nonnegative pseudo-spectrum function becomes a polynomial and the DF problem is reduced to a polynomial rooting problem [3,4], ESPRIT [2]. In case of a covariance-based RM algorithm, for an N-element array, the degree of the polynomial equals $2N-2$, so that $2N-2$ roots have to be calculated. In case of a fourth order (FO) statistics-based RM algorithm, the degree of the polynomial equals $4N-4$ and, consequently, $4N-4$ roots have to be calculated. For L incident signals, the directions of arrivals (DOA) are calculated from the L roots closest to the unit circle. This selection process can introduce serious errors in saturated[1] array environments, especially under low SNR and/or small sample size conditions because the signal roots then do not stay close to the unit circle. Unlike RM algorithms, reduced polynomial rooting (RPR) algorithms do not generate extraneous roots,[2] i.e., all polynomial roots correspond to the actual DOA. As is demonstrated in Section 4, this feature is of particular advantage in saturated array environments, especially in the case of FO methods when number of incident signals L exceeds number of elements N and low SNR and/or small sample size conditions and results in enhanced performance of RPR algorithms over RM algorithms.

The formulation of the RPR algorithms relies on the solution of an over-determined system of linear equations that yields the coefficients of an L degree polynomial. Depending on the required accuracy, this system can be solved either by using the Moore–Penrose pseudo-inverse or by using a more accurate total-least-square (TLS) approach [13]. Our numerical studies have shown that in not too demanding scenarios, where the separation between adjacent signals in the angular domain was not very close, the two approaches gave results of comparable accuracy. As will be demonstrated in Section 4, this computationally lighter version of the RPR algorithms is not inferior to RM algorithms. The RPR algorithms themselves are derived in Sections 2 and 3. Results of comparative performance evaluations are presented in Section 4. The conclusions are given in Section 5.

2. Linear antenna array model

Polynomial rooting-based super-resolution DF algorithms such as RM [3] offer computational efficiency in relation to the search-based DF methods [1] when the special geometry of the uniform linear arrays (ULA) is employed. In this case the problem of estimating the DOA of L signals incident on N-element array is described by

$$\mathbf{z}(t) = \mathbf{A}\mathbf{s}(t) + \mathbf{v}(t) \tag{1}$$

where $\mathbf{z}(t)$ is a complex column vector comprised of N signals at the output of the array; $\mathbf{A}$ is $N \times L$ steering matrix of the linear array comprised of the L column vectors $\mathbf{a}(\Omega_l)$ corresponding with the DOA of the l-th source signal; $\mathbf{s}(t)$ is a column vector comprised of the L source signals incident on the array and $\mathbf{v}(t)$ represents additive noise. If mutual coupling among the array elements is compensated [9] the steering vector for a ULA simplifies to

$$\mathbf{a}(\Omega_l) = \hat{f}(\Omega_l)[1 \;\; e^{jk_0 d\xi_l} \;\; e^{jk_0 2d\xi_l} \;\; \ldots \;\; e^{jk_0(N-1)d\xi_l}]^T \tag{2}$$

where $\Omega_l = (\theta_l, \varphi_l)$, $\xi_l = \sin(\theta_l)\cos(\varphi_l)$, θ_l and φ_l represent elevation and azimuth of the l-th source DOA, $k_0 = 2\pi/\lambda$ is a free space wave number evaluated at the receiver local oscillator frequency, λ is a wavelength, d is an inter-element spacing and $\hat{f}(\Omega_l)$ represents the element radiation pattern. In the formulation of the SO MUSIC algorithm [1] one estimates $\mathbf{E}_v$, the matrix of eigenvectors that span the noise subspace and forms the nonnegative function

$$\Lambda(\Omega) = \mathbf{a}(\Omega)^H \mathbf{E}_v \mathbf{E}_v^H \mathbf{a}(\Omega) \tag{3}$$

called pseudo-spectrum and employs the locations of its zeros to estimate the DOA's. For sufficiently large sample sizes the $\mathbf{E}_v$ can be well approximated by the eigenvectors of the sample data covariance matrix

$$\hat{\mathbf{R}}_{\mathbf{zz}} = (1/T)\sum_{t=1}^{T} \mathbf{z}(t)\mathbf{z}(t)^H$$

where 'H' denotes Hermitian operation. For the ULA in (2) the $\Lambda(\Omega)$ can be written in polynomial form [2] as follows:

$$\Lambda(z) = z^{-(N-1)} P_{2N-2}(z) \tag{4}$$

where $z = e^{jk_0 d\xi}$ and $P_{2N-2}(z)$ is the $2N-2$ degree polynomial in z. From (4) DOA are found from the L pairs of complex roots of the polynomial $P_{2N-2}(z)$ that are closest to the unit circle. The corresponding direction cosines are

$$\xi_l = angle(z_l)/k_0/d, \quad l = 1, 2, \ldots, L \tag{5}$$

In view of (4), RM requires the calculation of $2N-2$ roots. For large arrays this leads to high-computational loads and becomes a source of the numerical errors alluded to previously.

By analogy with the SO MUSIC pseudo-spectrum, the quadricovariance version is formulated as follows [10,11]:

$$\Lambda(\Omega) = (\mathbf{a}(\Omega) \otimes \mathbf{a}^*(\Omega))^H \mathbf{E}_v \mathbf{E}_v^H (\mathbf{a}(\Omega) \otimes \mathbf{a}^*(\Omega)) \tag{6}$$

[1] By a saturated array we refer to a scenario wherein the number of emitters L is close to either the number of real sensors N, in a case of the SO methods, or to the number of virtual sensors $2N-1$, in a case of the FO methods.

[2] We comment that RPR algorithms presented herein should not be confused with the algorithms we have recently derived in [16]. The latter algorithms rely on different subspace decomposition principles and require the solution of polynomials of order $2L$ instead of L and are, in that sense, computationally more demanding.

where $\otimes$ denotes tensorial or Kronecker's product, the '*' denotes the complex conjugate operation and $\mathbf{E}_v$ represents the matrix of eigenvectors that correspond to the noise subspace. They can be formally obtained from the eigenvalue decomposition of the $N^2 \times N^2$ sample data quadricovariance matrix $\mathbf{Q_{zz}}$ with the entries

$$Q_{zz}(r,q) = cum(z_i(t), z_k^*(t), z_l^*(t), z_m(t)) = \gamma_{4,s}(\Omega)\exp(\mathrm{j}(o-p)k_0 d\xi) \quad (7)$$

where $o = i+m$, $p = k+l$ and $\gamma_{4,s}$ represents FO cumulant of the incident signal $s(t)$ and the coordinates (r, q) are obtained from the mapping $C^4 \to C^2$ in accordance with the scheme $r = N(i-1)+k$, $q = N(l-1)+m$ where C^D denotes the field of complex numbers of dimension D. This mapping is necessary because quadricovariance is originally defined as a four-dimensional tensor [10]. However, the quadricovariance-based formulation of DF algorithms is computationally very demanding, requiring the estimation of N^4 FO cross-cumulants. At the same time, it is also redundant because the virtual array of $2N-1$ elements can be characterized by an $(2N-1)\times(2N-1)$ sample data covariance matrix instead of one of size $N^2 \times N^2$. Therefore, instead of using a quadricovariance-based formulation of the FO statistics-based DF algorithms, we shall exploit the minimum redundancy cumulant array (MRCA) concept [12] and formulate the covariance matrix of the virtual array of $2N-1$ elements using the identity

$$R_{vv}(v_n(t), v_m^*(t)) = \frac{\sigma_s^2}{\gamma_{4,s}} cum(z_i(t), z_j^*(t), z_k^*(t), z_l(t)) \quad (8)$$

with $n,m = 1,\ldots,2N-1$ and $i,j,k,l = 1,\ldots,N$. Because the constant $(\sigma_s^2/\gamma_{4,s})$ does not play a role in DF algorithms, we shall further simplify (8) to read

$$R_{vv}(v_n(t), v_m^*(t)) \;\Leftrightarrow\; cum(z_i(t), z_j^*(t), z_k^*(t), z_l(t)) \quad (9)$$

Exploiting (9), the formulation of the FO statistics-based version of either RM or RPR algorithm is straightforward, i.e., the SO statistics-based formulation of each algorithm is immediately applicable to FO statistics. Thus the FO pseudo-spectrum (6) can be written as follows:

$$\Lambda(\Omega) = \mathbf{a}_v^H(\Omega)\mathbf{E}_v\mathbf{E}_v^H\mathbf{a}_v(\Omega) \quad (10)$$

where $\mathbf{a}_v(\Omega)$ represents the steering vector of the virtual array and $\mathbf{E}_v$ represents the matrix of eigenvectors that correspond to the noise subspace. These can be obtained from the eigenvalue decomposition of the $(2N-1)\times(2N-1)$ sample data covariance matrix of the virtual array (9). This implies that approximately $N^2/4$ times fewer FO cross-cumulants have to be calculated when FO statistics-based DF algorithms are formulated using the equivalent covariance matrix of the virtual array instead of the quadricovariance matrix of the real array. Indeed, in view of the virtual array interpretation the FO pseudo-spectrum (10) reduces to

$$\Lambda(z) = z^{-2(N-1)}P_{4N-4}(z) \quad (11)$$

where $z = \mathrm{e}^{\mathrm{j}k_0 d\xi}$ and $P_{4N-4}(z)$ is the $4N-4$ degree polynomial in z. From (11) the DOA are found from the L pairs of complex roots of the polynomial $P_{4N-4}(z)$ that are closest to the unit circle, as in (5). Evidently the FO RM requires the calculation of $4N-4$ roots. Just as for SO RM, large arrays lead to high-computational loads creating potential sources of numerical error. The benefits of employing a FO over a SO-based formulation are in the extended aperture of the ULA and in the suppression of the additive Gaussian noise [12]. It is worth noting that the MRCA approach to FO statistics-based DOA estimation is structurally equivalent to the diagonal slice and contracted quadricovariance approaches introduced in [15], i.e., all three approaches avoid the estimation of the N^4 FO statistics. Asymptotic performance analysis of the FO methods has been presented in [15] for the MUSIC-like DOA estimation algorithm. As commented in more details in Section 4, numerically estimated DOA errors for SO and FO methods are consistent with the results of the asymptotic performance analysis presented in [15].

3. SO statistics-based RPR algorithm

From (1) and (2) the output signal $z_n(t)$ of the ULA is

$$z_n(t) = \sum_{l=1}^{L} \mathrm{e}^{\mathrm{j}nq\xi_l} s_l(t) + v_n(t), \quad n = 1,\ldots,N \quad (12)$$

where $q = k_0 d$. The data covariance matrix elements $R_{zz}(n,m)$ satisfy

$$R_{zz}(n,m) = \langle z_n(t) z_m^*(t)\rangle = \sum_{l=1}^{L}\sum_{k=1}^{L} \mathrm{e}^{\mathrm{j}(n\xi_l - m\xi_k)q} s_{lk} + \sigma^2\delta_{nm} \quad (13)$$

where $s_{lk} = \langle s_l(t)s_k^*(t)\rangle$, σ^2 represents the noise power and δ_{nm} is the Kronecker delta, i.e., it is assumed that additive noise is spatially white. Subtracting the noise constituent from the data covariance matrix in (13) we get

$$R_{zz}(n,m) - \sigma^2\delta_{nm} = \sum_{l=1}^{L}\sum_{k=1}^{L} \mathrm{e}^{\mathrm{j}(n\xi_l - m\xi_k)q} s_{lk} \equiv w_{nm} \quad (14)$$

Now consider an $L+1$-dimensional column vector $\mathbf{c}$

$$\mathbf{c} = [c_1 \;\; c_2 \;\; \cdots \;\; c_{L+1}]^{\mathrm{T}} \quad (15)$$

and construct the following product with the right side of (14):

$$\sum_{p=1}^{L+1} w_{np}c_p = \sum_{l=1}^{L}\sum_{k=1}^{L} \mathrm{e}^{\mathrm{j}nq\xi_l}\langle s_l s_k^*\rangle \mathrm{e}^{-\mathrm{j}q\xi_k} \sum_{p=1}^{L+1} \mathrm{e}^{-\mathrm{j}(p-1)q\xi_k} c_p \quad n = 1,2,\ldots,N \quad (16)$$

We now seek a solution to the homogeneous system

$$\sum_{p=1}^{L+1} w_{np}c_p = 0 \quad (17)$$

Since the matrix with elements $\langle s_l s_k^*\rangle$ is positive definite (assuming linearly independent signals) (17) will possess nontrivial solutions if and only if

$$\sum_{p=1}^{L+1} \mathrm{e}^{-\mathrm{j}(p-1)q\xi_k} c_p = 0 \quad (18)$$

Evidently this corresponds to the zeros of the L-th order polynomial

$$P_L(z) = \sum_{p=1}^{L+1} c_p z^{p-1} = \sum_{r=0}^{L} c_{r+1} z^r \tag{19}$$

at $z = e^{-jq\xi_k}$. Thus the L DOA can be calculated from the roots of the polynomial $P_L(z)$ in a manner analogous to (5). Since c_1 in (18) can be chosen arbitrarily we may set $c_1 = -1$ so that (18) becomes

$$\sum_{p=2}^{L+1} w_{np} c_p = w_{n1}, \quad n = 1, 2, \ldots, N \tag{20}$$

Eq. (20) can be written in matrix form

$$\mathbf{W}\mathbf{c}_p = \mathbf{w}_1 \tag{21}$$

where $\mathbf{w}_1$ is first column vector of the $N \times N$ matrix defined by the double sum in (14) and $\mathbf{W}$ is comprised of columns $2 \ldots L+1$, i.e.,

$$\mathbf{W} = [\mathbf{w}_2 \ \ \ldots \ \ \mathbf{w}_{L+1}] \tag{22}$$

where $\mathbf{w}_2, \ldots, \mathbf{w}_{L+1}$ are column vectors and $\mathbf{c}_p$ is a column vector defined as

$$\mathbf{c}_p = [c_2 \ \ \ldots \ \ c_{L+1}]^{\mathrm{T}} \tag{23}$$

Eq. (21) represents an over-determined system of linear equations. Note that the matrix elements w_{nm} are ensemble averages that in practice cannot be determined exactly. Instead they must be replaced by estimates $\hat{w}_{np}$ obtained from the eigenanalysis of the sample covariance matrix $\hat{\mathbf{R}}_{zz}$. To make this notationally explicit we replace (20) by the approximate form

$$\sum_{p=2}^{L+1} \hat{w}_{np} c_p \approx \hat{w}_{n1}, \quad n = 1, 2, \ldots, N \tag{24}$$

Eq. (24) is best solved in the LMS sense using either TLS [13] or the LMS formulation using the singular value decomposition (Moore–Penrose pseudo-inverse). The DOA are then estimated from the roots of the polynomial (19) with the coefficients defined by the vector

$$\mathbf{c} = [-1 \ \ \mathbf{c}_p^{\mathrm{T}}]^{\mathrm{T}} \tag{25}$$

The derivation of the FO statistics version of RPR algorithm is straightforward: the same algorithm is simply applied on the sample data covariance matrix of the virtual array R_{vv} given by (9).

At this point we would like to comment on the relation between the SO RPR algorithm and the iterative quadratic maximum-likelihood (IQML) algorithm of [14], as well as on the relation between the FO RPR algorithm and the FO statistics-based minimum variance algorithm described in [11]. Both SO RPR and IQML algorithms estimate DOAs from the L roots of the L-th order polynomial. However, in our algorithm the polynomial coefficients are determined by solving the over-determined system of linear equations (21) by means of either Moore–Penrose pseudo-inverse or TLS. In the IQML method the coefficients are found via an iterative procedure that involves the solution of a quadratic minimization problem at each iteration step. Similarly, in case of the FO statistics-based minimum variance algorithm [11] the DOAs are found as solutions of a nonlinear optimization problem with accuracy slightly better than obtained by MUSIC-like FO methods [11]. Here, we have shown that thanks to the MRCA concept,

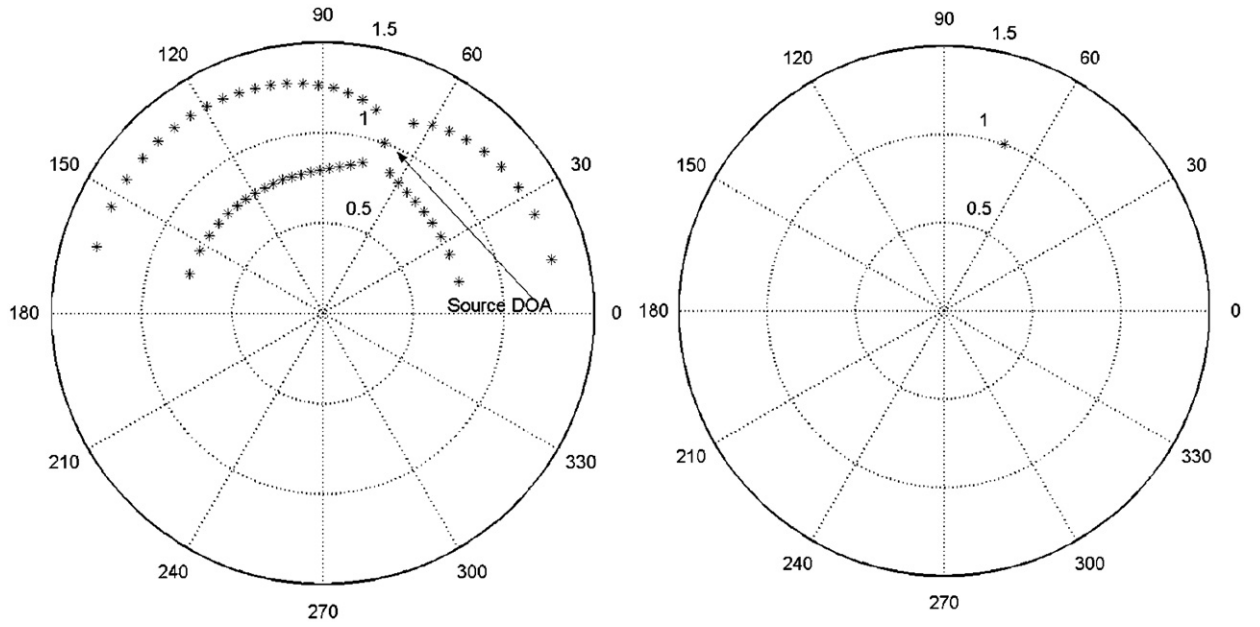

Fig. 1. DOA estimated by SO RM algorithm (left) and RPR algorithm (right) for one source impinging from 70° on 30-element ULA.

the FO RPR algorithm retains the same algebraic simplicity as the SO RPR algorithm and is computationally much simpler than FO minimum variance method proposed in [11].

4. Numerical results

In this section we systematically evaluate numerically the performance of the SO and FO RPR and RM algorithms. All results produced by RPR algorithms are obtained by using the Moore–Penrose pseudo-inverse so that the RPR algorithm retains its simple computational structure. We mention that we have also employed the TLS-based versions in all the examples reported herein and the results were not significantly different from the Moore–Penrose pseudo-inverse approach.

In Fig. 1 we compare the performance of the SO RM and SO RPR algorithms for a single signal incident at 70° on a

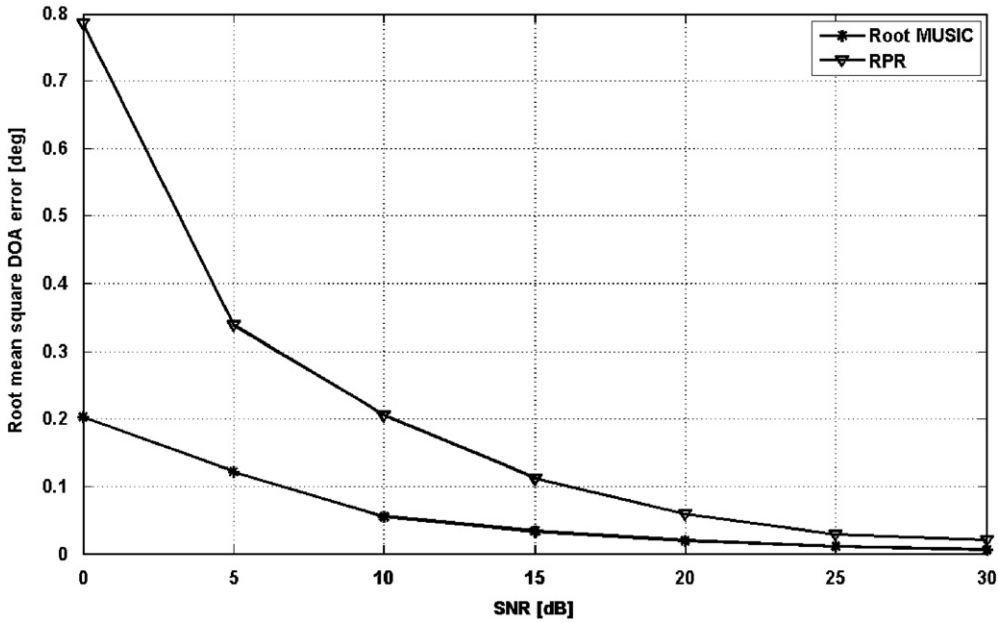

Fig. 2. RMSE error vs. SNR value for one source impinging from 70° on four-element ULA. Data record length was 1000 samples. SO RM algorithm '*' and SO RPR algorithm '∇'.

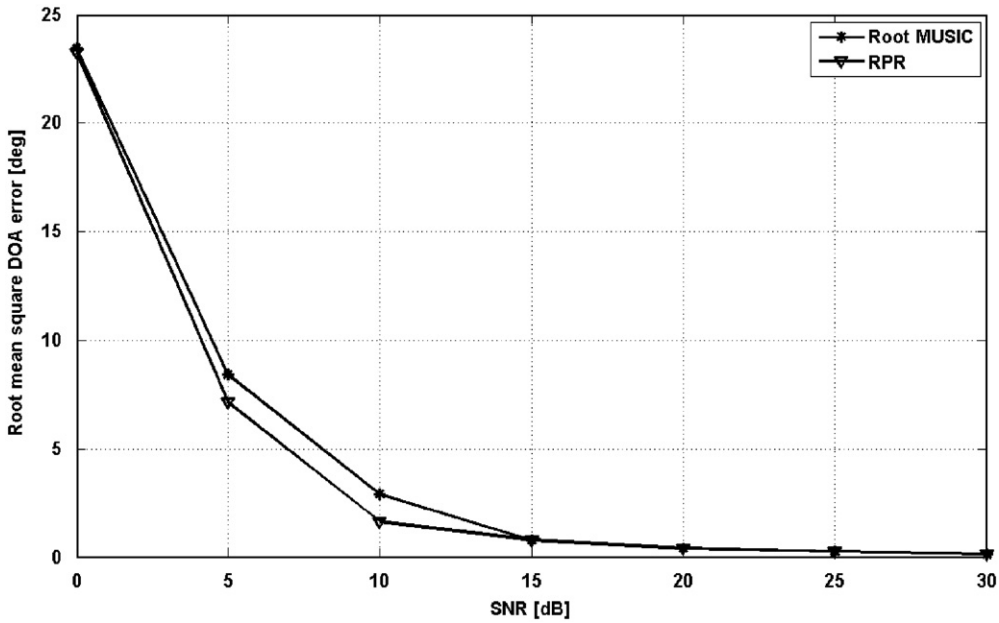

Fig. 3. RMSE error vs. SNR value for three sources impinging from directions of 30°, 50° and 70° on four-element ULA. Data record length was 1000 samples. SO RM algorithm '*' and SO RPR algorithm '∇'.

30-element ULA with an inter-element spacing of $\lambda/2$. The sample size was 10 000 and SNR = 25 dB. The root locus diagram associated with the estimated DOA positions for RM is shown on the left of side of Fig. 1 and for the RPR algorithm on right. The DOA estimation error for both algorithms was less than 0.01°. However, while RM algorithm required calculation of $2N-2=58$ roots, only one root had to be calculated by the RPR algorithm. In Figs. 2 and 3 we compare the accuracy of the SO RPR and SO RM algorithms in terms of the root mean square error (RMSE) as a function of the SNR for one and three signals incident on a four-element ULA from directions of 70° and (70°, 50°, 30°), respectively. The sample size was 1000. While RM algorithm shows better performance for one source, the RPR algorithm shows better performance for three sources. Equivalent conclusions can be drawn from

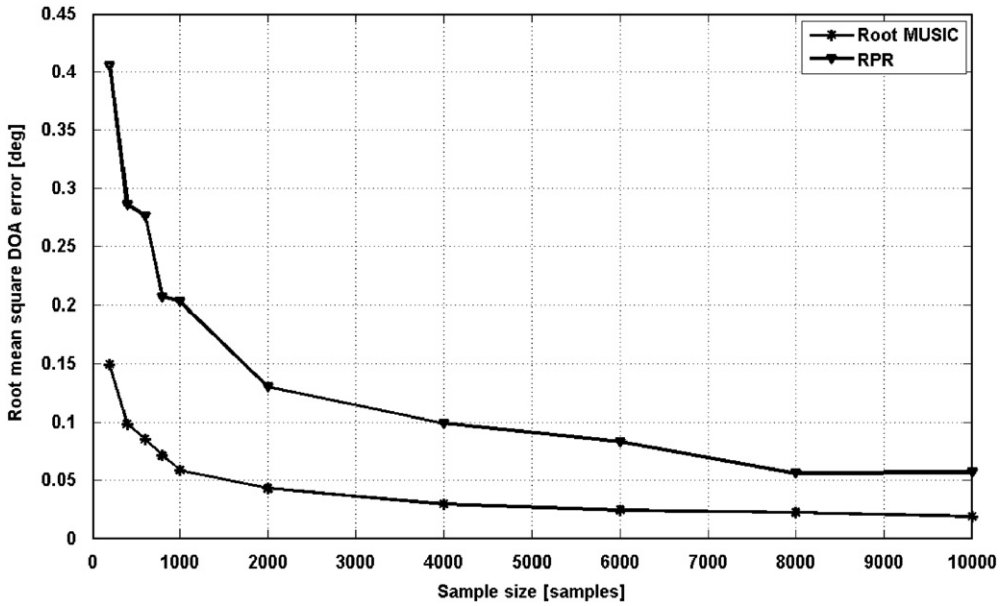

Fig. 4. RMSE error vs. sample size value for one source impinging from 70° on four-element ULA. SNR value was 10 dB. SO RM algorithm '*' and SO RPR algorithm '∇'.

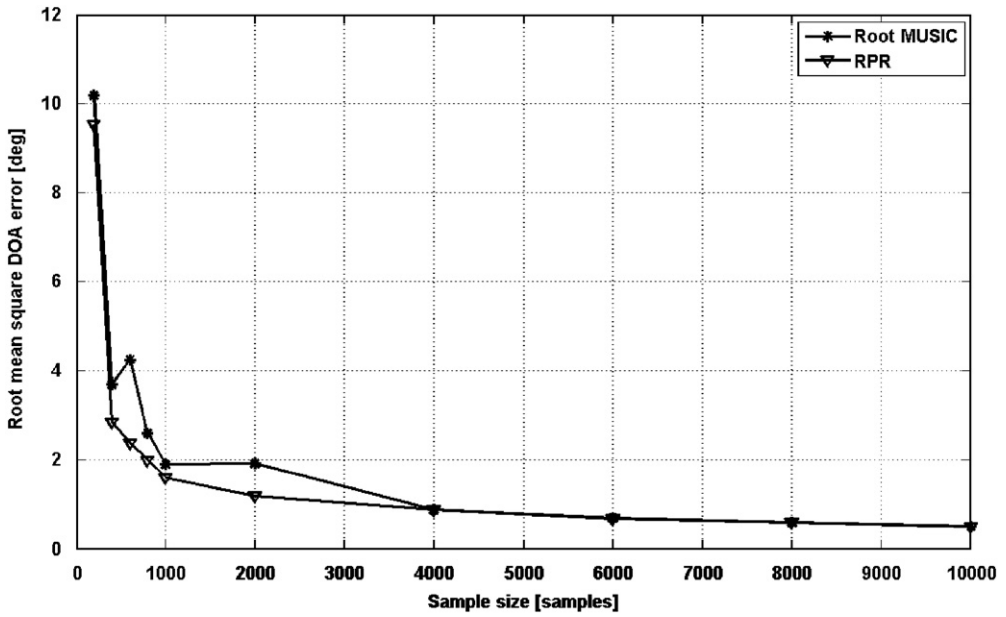

Fig. 5. RMSE error vs. sample size value for three sources impinging from directions of 30°, 50° and 70° on four-element ULA: SNR value was 10 dB. SO RM algorithm '*' and SO RPR algorithm '∇'.

an examination of Figs. 4 and 5, which show the RMSE as a function of the sample size for both algorithms for one and three sources, respectively and an SNR of 10 dB. In all examples the RMSE was derived using 100 runs. Figs. 3 and 5 corroborate our statement that extraneous roots, characteristic of the RM algorithm, cause errors in the scenarios that involve either low SNR or a saturated array.

In Figs. 6–9 we illustrate the performance of FO RPR and FO RM algorithms. In Fig. 6 one signal is impinging from 70° on a 10-element ULA with an inter-element spacing of $\lambda/2$. The sample size was 10 000 and SNR = 25 dB. The root locus diagram for the FO statistics-based RM algorithm is shown on the left side of Fig. 6 and for the FO statistics-based RPR algorithm on the right side. The DOA error for both algorithms was less than 0.01°. However,

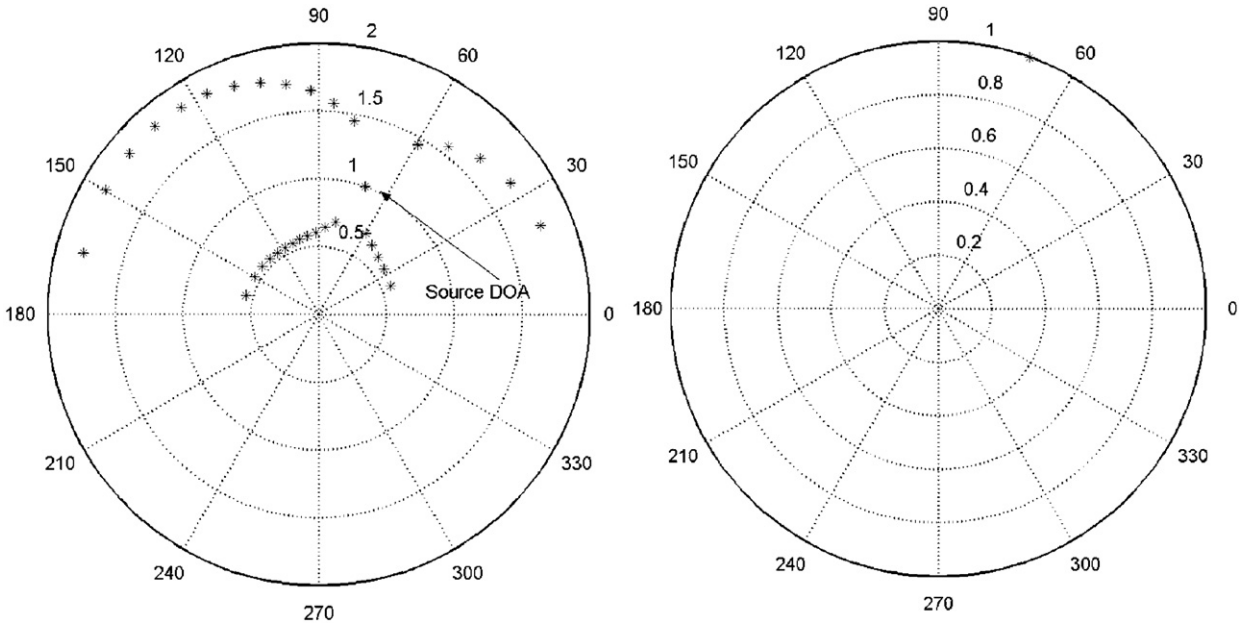

Fig. 6. DOA estimated by FO RM algorithm (left) and FO RPR algorithm (right) for one source impinging from 70° on 10-element ULA.

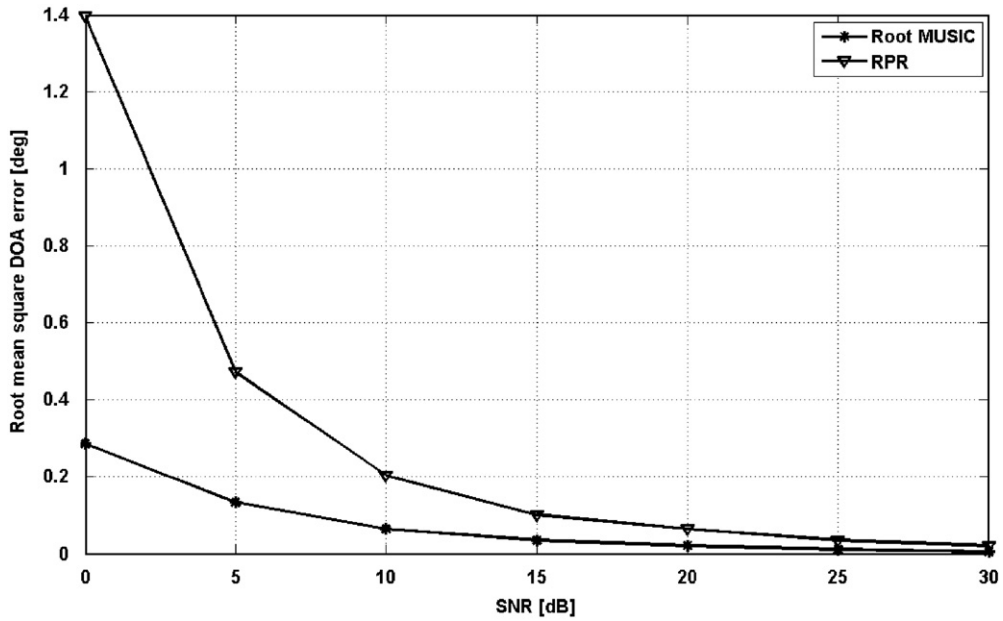

Fig. 7. RMSE error vs. SNR value for one source impinging from 70° on four-element ULA. Data record length was 1000 samples. FO RM algorithm '*' and FO RPR algorithm '∇'.

while RM algorithm required calculation of $4N-4=36$ roots, only one root had to be calculated by the RPR algorithm. Figs. 7–9 show the RMSE as a function of the SNR for one, three and six signals impinging on a four-element ULA from directions of 70°, (70°,50°,30°) and (130°, 110°, 90°, 70°, 50°, 30°), respectively. The sample size was again 1000. Similarly to SO RPR, RM exhibited slightly better performance for one source, but the RPR exhibited significantly better performance for six sources. For three sources RM performed better under low-SNR conditions. The seemingly illogical results shown in Fig. 9, where the RMSE error of the FO RM algorithm is

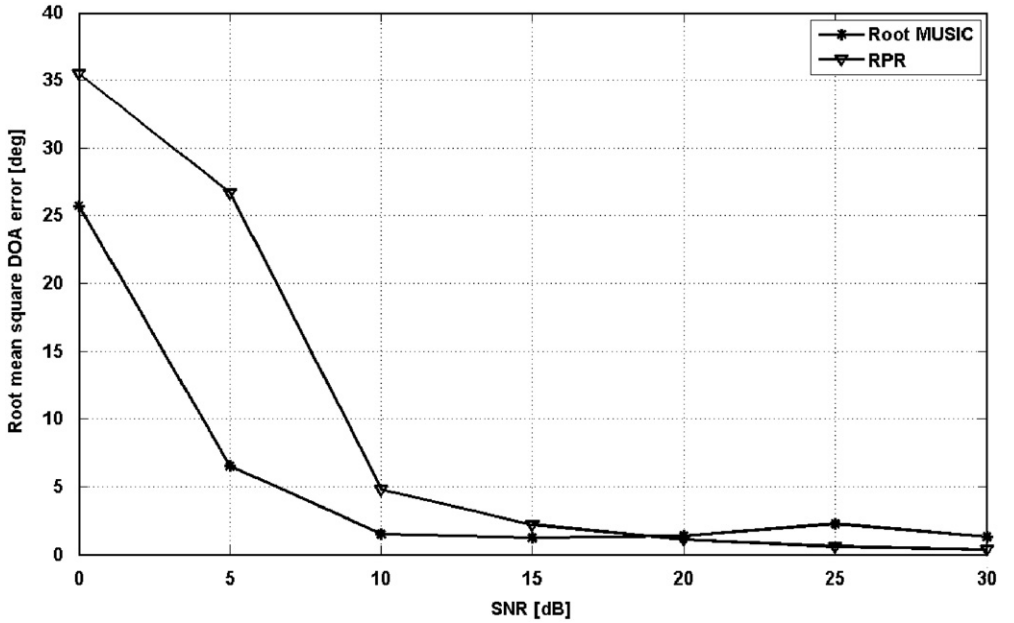

Fig. 8. RMSE error vs. SNR value for three sources impinging from directions of 30°, 50° and 70° on four-element ULA. Data record length was 1000 samples. FO RM algorithm '*' and SO RPR algorithm '∇'.

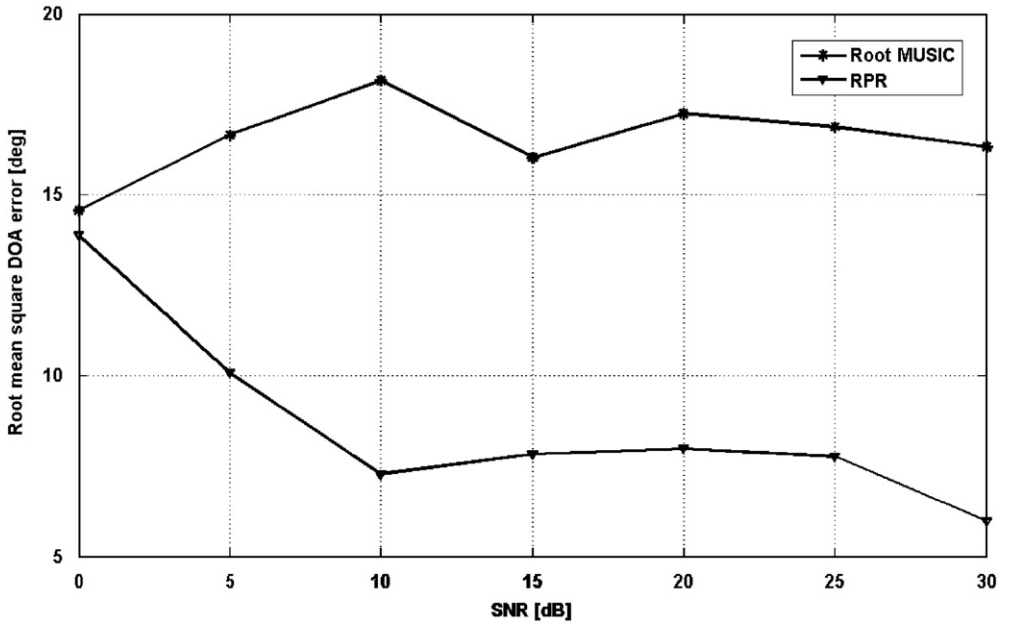

Fig. 9. RMSE error vs. SNR value for six sources impinging from directions of 130°, 110°, 90°, 70°, 50° and 30° on four-element ULA. Data record length was 1000 samples. FO RM algorithm '*' and FO RPR algorithm '∇'.

increasing with the increasing SNR, is explained by the presence of extraneous roots characteristic of the RM. When array is over-saturated, i.e., when the number of emitters is greater than number of real sensors, the roots corresponding to the real emitters do not stay close to the unit circle and it can be difficult to distinguish them from the extraneous roots. This is especially true when the SNR becomes low. To support this statement we show in Fig. 13 seven pairs of roots generated by the FO RM algorithm for six incident signals with SNR = 0 dB. Evidently extraneous roots close to 150° are closer to the unit circle than the roots corresponding to the real signal at 130°. A conclusion equivalent to the one that may be drawn from the plots in Figs. 7–9 can also be drawn from an examination of Figs. 10–12, which show the RMSE as a function of the sample size for both algorithms for the case of one, three and six sources, respectively (see Fig. 13). The SNR was 10 dB. These numerical results are consistent with

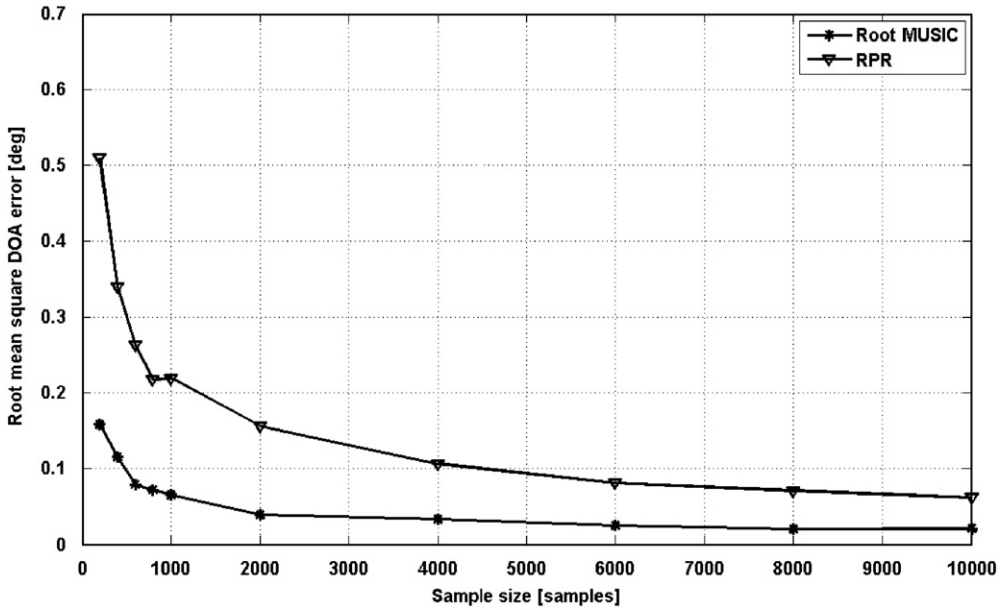

Fig. 10. RMSE error vs. sample size value for one source impinging from 70° on four-element ULA. SNR value was 10 dB. FO RM algorithm '*' and FO RPR algorithm '∇'.

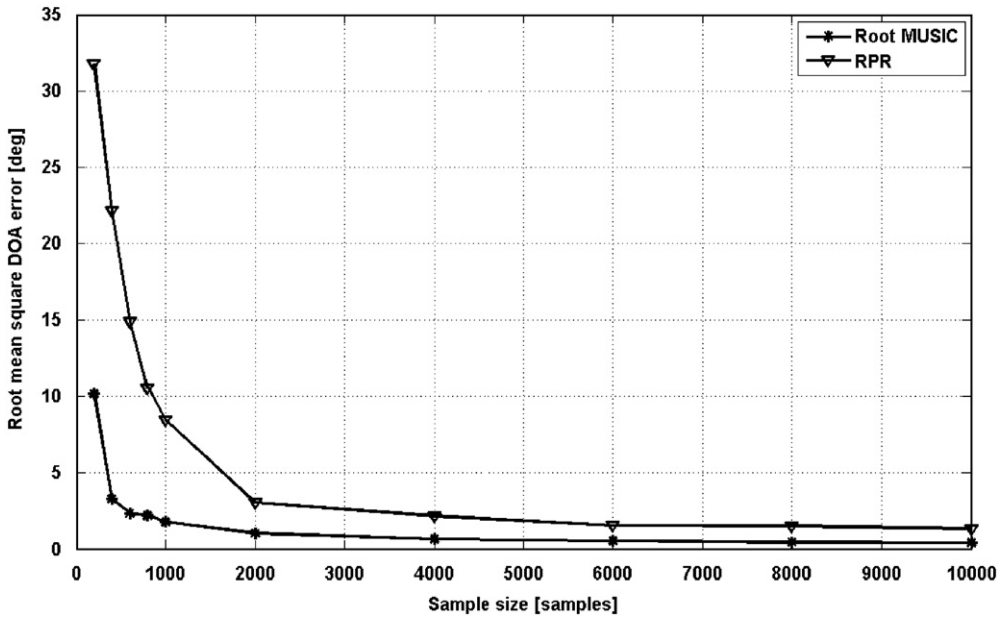

Fig. 11. RMSE error vs. sample size value for three sources impinging from directions of 30°, 50° and 70° on four-element ULA. SNR value was 10 dB. FO RM algorithm '*' and FO RPR algorithm '∇'.

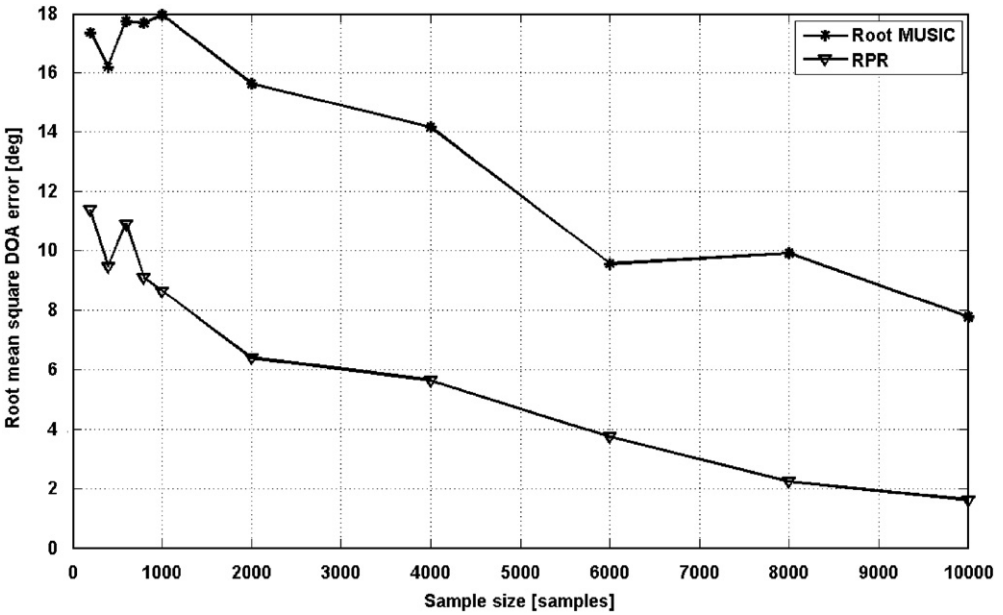

Fig. 12. RMSE error vs. sample size value for six sources impinging from directions of 130°, 110°, 90°, 70°, 50° and 30° on four-element ULA. SNR value was 10 dB. FO RM algorithm '*' and FO RPR algorithm '∇'.

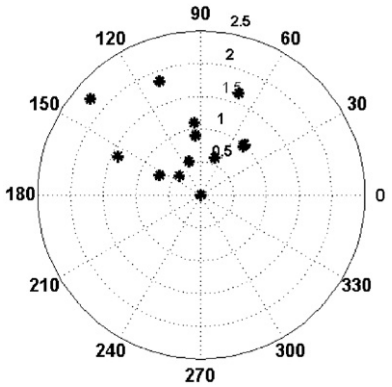

Fig. 13. Root locus diagram generated by FO RM algorithm with six sources impinging from directions of 130°, 110°, 90°, 70°, 50° and 30° on the four-element ULA. Data record length was 1000 samples and SNR = 0 dB.

asymptotic performance analysis of the SO and FO MUSIC algorithm, [15], i.e., SO and FO method exhibit similar performance for high SNR. However, at low SNR, the variance of the DOA estimate grows as the fourth power of the inverse of the SNR for FO methods and with the power of two for SO methods. This, for example, explains results shown in Figs. 3 and 8.

5. Conclusions

The number of roots that must be calculated for SO and FO statistics-based RM algorithms is, respectively $2N-2$ and $4N-4$. In addition to increasing the computational load, the extraneous roots necessarily present in RM type algorithms lead to poor performance in saturated array environments and under low SNR and/or small sample size conditions. For the novel SO and FO statistics-based RPR algorithms presented in this paper, the number of roots that needs to be calculated equals precisely to the number of incident signals. Consequently, for large arrays, RPR algorithms can lead to a significant reduction of the computational load and, as shown in this paper, indirectly, to a reduction of numerical errors in DOA estimation. It is demonstrated through numerical simulations that in saturated array environments, especially in the case of FO methods when number of incident signals L exceeds number of elements N and low SNR and/or small sample size conditions the RPR algorithms significantly outperform the RM algorithms.

References

[1] R.O. Schmidt, A signal subspace approach to multiple emitter location and spectral estimation, Ph.D. Dissertation, Stanford University, 1981.
[2] R. Roy, T. Kailath, ESPRIT—estimation of signal parameters via rotational invariance techniques, IEEE Transactions on Acoustics, Speech, and Signal Processing 37 (7) (1989) 984–995.
[3] A.J. Barabell, Improving the resolution performance of eigenstructure-based direction-finding algorithms, in: Proceedings of the IEEE International Conference Acoustics Speech and Signal Processing, Boston, MA, 1983, pp. 336–339.
[4] B.D. Rao, K.V.S. Hari, Performance analysis of Root-MUSIC, IEEE Transactions on Acoustics, Speech, and Signal Processing 34 (12) (1989) 1939–1949.
[5] H. Abdallah, W. Wasylkiwskyj, K. Parikh, A. Zaghloul, Comparison of return loss calculations with measurements of narrow-band microstrip patch antennas, The Applied Computational Electromagnetics Journal 19 (3) (2004) 184–187.
[6] C. Roller, W. Wasylkiwskyj, Effects of mutual coupling on superresolution in DF linear arrays, in: Proceedings of the IEEE

International Conference Acoustics Speech and Signal Processing, San Francisco, CA, 1992, pp. V257–V260.
[7] W. Wasylkiwskyj, I. Kopriva, Equalization of the element radiation patterns for root based direction finding algorithms, in: Proceedings of the 2004 URSI Symposium on Electromagnetic Theory, vol. I, Pisa, Italy, May 23–27, 2004, pp. 364–366.
[8] S. Lundgren, A study of mutual coupling effects on the direction finding performance of ESPRIT with a linear microstrip patch array using the method of moments, in: Proceedings of the IEEE AP-S Symposium, Baltimore, July 1996, pp. 1372–1375.
[9] H. Steyskal, J.S. Herd, Mutual coupling compensation in small array antennas, IEEE Transactions on Antennas and Propagation 38 (12) (1990) 1971–1975.
[10] P. Chevalier, A. Ferreol, On the virtual array concept for the fourth-order direction finding problem, IEEE Transactions on Signal Processing 47 (9) (1999) 2592–2595.
[11] B. Porat, B. Friedlander, Direction finding algorithms based on high-order statistics, IEEE Transactions on Signal Processing 39 (9) (1991) 2016–2024.
[12] M.C. Dogan, J.M. Mendel, Applications of cumulants to array processing—part I: aperture extension and array calibration, IEEE Transactions on Signal Processing 43 (5) (1995) 1200–1216.
[13] G.H. Golub, C.F. Van Loan, An analysis of the total least squares problem, SIAM Journal on Numerical Analysis 17 (1980) 883–893.
[14] Y. Bresler, A. Macovski, Exact maximum likelihood parameter estimation of superimposed exponential signals in noise, IEEE Transactions on Acoustics, Speech, and Signal Processing 34 (5) (1986) 1081–1089.
[15] J.F. Cardoso, E. Moulines, Asymptotic performance analysis of direction-finding algorithms based on fourth-order cumulants, IEEE Transactions on Signal Processing 43 (1) (1995) 214–224.
[16] W. Wasylkiwskyj, I. Kopriva, M. Doroslovački, A.I. Zaghluol, A new root-based direction finding algorithm, Radio Science 42 (2007) RS2S90.